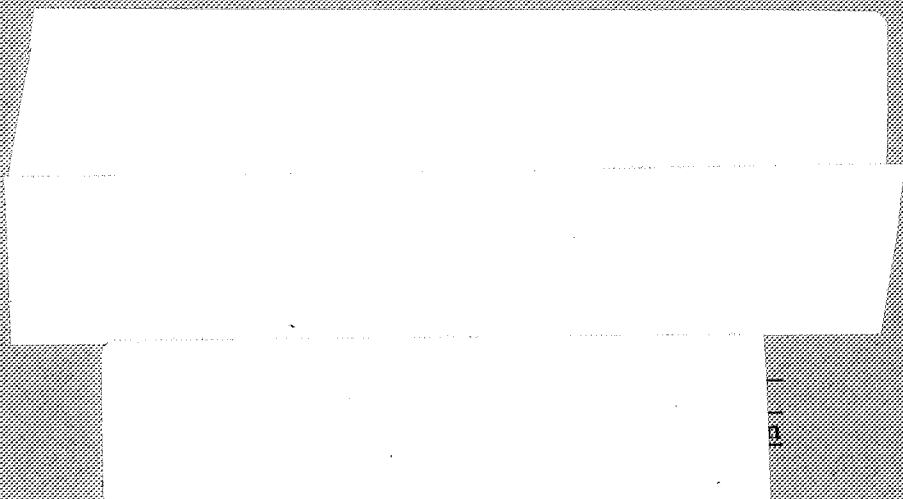


NASA Technical Paper 1617

**Compression Panel Studies
for Supersonic Cruise Vehicles**

**Robert R. McWithey, Dick M. Royster,
and William L. Ko**

MARCH 1980



NASA

NASA Technical Paper 1617

Compression Panel Studies for Supersonic Cruise Vehicles

Robert R. McWithey and Dick M. Royster
Langley Research Center
Hampton, Virginia

William L. Ko
Dryden Flight Research Center
Edwards, California



National Aeronautics
and Space Administration

**Scientific and Technical
Information Office**

1980

SUMMARY

Results of analytical and experimental studies are summarized for titanium, boron-fiber-reinforced aluminum-matrix composite, Borsic¹-fiber-reinforced aluminum-matrix composite, and titanium-sheathed Borsic-fiber-reinforced aluminum-matrix composite stiffened panels. The results indicate that stiffened panels with continuous joints (i.e., brazed, diffusion-bonded or adhesive-bonded joints) are more structurally efficient than geometrically similar panels with discrete joints (i.e., spotwelded or bolted joints). In addition, results for various types of fiber-reinforced aluminum-matrix stiffened panels indicate that titanium-sheathed Borsic-fiber-reinforced aluminum-matrix composite panels are the most structurally efficient. Analytical results are also presented for graphite-fiber-reinforced polyimide-matrix composite stiffened panels and superplastically formed and diffusion-bonded titanium sandwich panels.

INTRODUCTION

Analytical studies (refs. 1, 2, and 3) indicate that significant gains in supersonic-cruise vehicle performance are possible by the use of advanced-composite primary structures made of boron-fiber-reinforced aluminum-matrix composite (B/Al) and/or graphite-fiber-reinforced polyimide-matrix composite (Gr/PI) materials in place of conventional titanium structures. In addition, some of these and other studies (refs. 4 and 5) indicate that the use of composite-reinforced conventional titanium structures and superplastically formed and diffusion-bonded (SPF/DB) titanium structures can also offer significant gains in vehicle performance compared to conventional titanium structures. The results of these studies are partially based on the assumption that the buckling behavior of composite compression panels and SPF/DB titanium panels is reliably predicted by buckling analyses developed for panels fabricated from conventional materials. Furthermore, knowledge of the effects of fabrication techniques on the buckling behavior of panels fabricated from these advanced materials was limited.

The purpose of the present paper is to summarize results from several studies conducted on candidate structural materials (i.e., titanium, B/Al, Borsic-fiber-reinforced aluminum-matrix composite (Bsc/Al), titanium-sheathed Bsc/Al (ticlad Bsc/Al), and Gr/PI) for supersonic-cruise vehicles to evaluate the effects of fabrication and joining processes, and material properties on panel buckling behavior. Effects of joining processes on the buckling behavior of hat-stiffened titanium panels were investigated during the

¹Borsic: Registered trade name of United Aircraft Products, Inc.

development of the weld-braze joining process (ref. 6). Subsequent studies (refs. 7 and 8) investigated the effects of stiffener fabrication processes (hot and cold forming, and eutectic bonding) and joining processes (bolting, adhesive bonding, diffusion bonding, spotwelding, and brazing) on the structural efficiency of aluminum-matrix compression panels.

In addition, the results of analytical studies conducted on composite and selectively reinforced titanium stiffened panels (refs. 9 and 10), and SPF/DB titanium expanded sandwich panels (ref. 11), identified structurally efficient panel designs. Several designs were subsequently selected for fabrication and testing to determine their buckling and failure characteristics. Results from these analytical studies and available test data for these panels are also presented in this paper.

The use of trade names in this paper does not constitute official endorsement, either expressed or implied, by the National Aeronautics and Space Administration.

SYMBOLS

A	panel planform area
a	sandwich panel length
b	stiffened panel element width
c	sandwich panel width
E	modulus of elasticity of sandwich panel material
E_{22}	transverse modulus of unidirectional composite material
I	moment of inertia per unit width of face sheets taken about sandwich middle surface
L	stiffened panel length
N_x	uniaxial buckling stress resultant
P	buckling load
P_{cr}	maximum analytical buckling load used to normalize data in figure 4
P'_{cr}	analytical buckling load based on reduced modulus
t	stiffened panel element thickness
W	panel mass
x,y,z	panel coordinate system

TEST METHODS

Panels with a single hat stiffener were used to evaluate fabrication and joining processes by determining the effects of these processes on panel local buckling loads and panel failure loads. A typical panel configuration used in these evaluations is shown in figure 1. The panels were tested at room temperature in uniaxial compression using a standard testing machine with the unloaded edges simply supported. Loaded ends of the panel were potted (see fig. 1) to prevent brooming during testing and to facilitate machining the ends flat and parallel.

Panels with three hat stiffeners were used in tests to determine local buckling characteristics and failure loads of structurally efficient panel designs. The test methods used were similar to those used to evaluate fabrication and joining processes except the unloaded edges of the three-stiffener panels were unsupported. A 6061 aluminum alloy was used as the matrix material in all aluminum-matrix panels.

FABRICATION AND JOINING STUDIES

Weld-Brazed Titanium

During the development of the weld-braze joining process described in reference 6, groups of geometrically identical hat-stiffened panels were fabricated from Ti-6Al-4V alloy with the hat stiffener attached to the skin by riveting, spotwelding, or weld-brazing. In the weld-braze process the stiffener is initially attached to the skin using several spotwelds along the length of both attachment flanges. Braze material is then positioned along the sides of the attachment flanges. During the braze heat cycle, braze material flows between the attachment flanges and skin because of capillary action, ultimately forming a continuous bond between the skin and attachment flanges.

Test results, from reference 6, are shown in figure 2 where buckling and failure stresses are plotted as a function of the web b/t ratio. These results indicate that continuously bonded weld-brazed panels have significantly higher buckling and failure stresses than discretely attached riveted and spotwelded panels. The significant improvement in structural efficiency of the weld-brazed panels gives insight into the effects of fabrication and joining processes on the buckling behavior of aluminum-matrix composites. The results of these studies are described in the next section.

Aluminum-Matrix Composites

Because significant differences exist in material behavior between aluminum-matrix composites and the nearly isotropic behavior of titanium, a comprehensive fabrication and joining study was performed on aluminum-matrix composites using the materials and fabrication and joining processes shown in Table I. Details of the fabrication and joining processes and test results are given in references 7 and 8.

Effects of fabrication processes. - Hat stiffeners fabricated using the hot or cold forming process were fabricated from preconsolidated flat sheet material. Because of bending limitations of the fibers in the preconsolidated sheet, the hot and cold forming processes required that fibers be oriented in only the longitudinal direction of the stiffeners. The eutectic consolidation process, on the other hand, allowed the stringers to be fabricated directly from monolayer B/Al material, thus providing a possible means for introducing cross-ply material into the stiffener webs for better structural efficiency. All stiffeners in the study, however, contained only longitudinally oriented fibers.

Test results indicate the panels with stiffeners fabricated using the eutectic consolidation process usually exhibit lower buckling and ultimate strengths than similar panels with hot or cold formed stiffeners. Furthermore, fiber bending tests indicate a 25-percent decrease in strength for fibers subjected to the eutectic consolidation process. Fiber strength was unaffected by the hot or cold forming processes used in forming the stiffeners, and the tests indicated no significant differences in strengths of similar panels with stiffeners fabricated using these processes.

Effects of joining processes.- The joining processes were chosen to provide a comparison between discrete-fastener and continuous-joining methods of attaching the stiffener to the skin. Brazing was not considered a feasible process for joining B/Al because of anticipated fiber degradation due to interaction with the matrix during the braze temperature cycle.

The effects of joining process on the buckling stress of the B/Al and Bsc/Al panels are shown in figure 3. The same buckling stress was obtained with discretely attached spotwelded or bolted B/Al panels, whereas the buckling stress of continuously adhesive-bonded or diffusion-bonded B/Al panels was 30 percent higher. Results from a spotwelded Bsc/Al panel test indicated a buckling stress nearly equal to the buckling stress of the spotwelded B/Al panels. In contrast to the 30-percent increase in B/Al panel buckling stress, only a 9-percent increase in buckling stress was observed in the continuously bonded (braze) Bsc/Al panels. Metallurgical examination of cross sections of the braze joint and results of fiber bending tests produced evidence of fiber degradation due to the braze process. Parallel studies (refs. 12 and 13) indicated that successful braze joints can be made with a minimum of fiber and matrix degradation using 1100 aluminum alloy as an outer layer on the composite that serves as a diffusion barrier between the braze and the matrix. This diffusion barrier concept was improved by use of titanium foil as an outer layer (ticlad Bsc/Al) as described in reference 8.

The ticlad Bsc/Al concept offers distinct advantages over Bsc/Al. Ticlad Bsc/Al prevents degradation of the fiber and matrix in the Bsc/Al laminate during the braze temperature cycle and provides a durable surface that reduces the possibility of surface damage during handling. In addition, the consolidated ticlad Bsc/Al flat sheet with unidirectional fibers can be hot formed into structural shapes, but the fibers must remain straight during the forming process. Additional advantages derived from the use of ticlad Bsc/Al are improvements in shear and transverse stiffness properties over those of the unclad unidirectional Bsc/Al laminate. In laminates with

unidirectional fibers, both of these properties are matrix controlled in a Bsc/Al laminate and are controlled by the titanium in a ticlad Bsc/Al laminate.

Comparison of analytical and experimental results. - Panel buckling loads and mode shapes obtained from fabrication and joining evaluation tests were compared with analytical results for each panel. Analytical results were obtained from the BUCLASP 2 computer program (ref. 14) using measured panel dimensions. Material property data used in the analyses are given in Table II. A comparison between analytical and experimental results is given in figure 4 for panels with continuous joints where buckling load P is normalized by the maximum analytical buckling load P_{cr} , obtained using the material property data given in Table II, for each of the five combinations of skin and stiffener materials shown in Table I. Three values of the ratio P/P_{cr} are shown for each type of panel and represent values of P obtained from

1. Analysis using the material property data given in Table II ($P/P_{cr}=1$).

2. Analysis using the material property data in Table II except at the corner elements of the attachment flange (see fig. 4) where a value of $E_{22} = 10.3$ GPa (ref. 15) was used for the corner elements instead of 131 GPa. (Not used for the ticlad Bsc/Al panel.)

3. Experiment.

Examination of the analytical and experimental results indicates similar mode shapes for all panel data shown in figure 4. For the panels containing unclad Bsc/Al, the mode shapes indicated that considerable bending is present at the corners of the stiffeners adjacent to the attachment flanges. Furthermore, examination of the transverse stress-strain curve for unidirectional Bsc/Al indicates plastic behavior occurs at a very low strain level. Therefore, a reduced transverse modulus ($E_{22} = 10.3$ GPa) corresponding to a strain level of approximately 0.002 (see ref. 15) was used in these corner elements and the panels containing the unclad Bsc/Al were again analyzed using BUCLASP 2. The results indicated that the panel buckling load P'_{cr} was significantly reduced without alteration of the mode shape. These buckling load results are shown in figure 4 and indicate good agreement between the analytical buckling loads with the reduced modulus in the corner elements and experimental buckling loads. For the ticlad Bsc/Al panel, figure 4 indicates that good agreement was obtained between analytical and experimental buckling loads when the value of $E_{22} = 131$ GPa was used for the entire panel and indicates that experimental buckling loads of ticlad Bsc/Al panels nearly attain analytical predictions without a reduced modulus in the analysis.

Slightly poorer agreement between the analytical and experimental buckling loads was obtained for the spotwelded panels. This lack of agreement occurs because the analysis program only has the capability to model a continuous joint along the panel length and thus cannot account for the effects of discrete fasteners.

Gr/PI Composites and SPF/DB Titanium

Fabrication and joining studies on Gr/PI composites are being performed under the CASTS program (Composites for Advanced Space Transportation Systems) and some results of these studies are presented in reference 16. Although the structural and thermal requirements for the CASTS program differ from those for supersonic cruise, the fabrication and joining studies from CASTS are believed applicable to the cruise requirement. Fabrication and joining studies on SPF/DB titanium are currently being conducted. Some results from these studies are given in reference 17.

COMPRESSION PANEL STUDIES

While the fabrication and joining methods were being developed and evaluated, analytical studies were conducted to develop structurally efficient stiffened panel designs for the combinations of material, stiffeners, and skins shown in figure 5. An optimization computer program incorporating a simplified buckling analysis was used to design the titanium, Bsc/Al, and ticlad Bsc/Al panels. An optimization program containing a refined buckling analysis and entitled PASC0, which was developed after the designs were established for the titanium, Bsc/Al and ticlad Bsc/Al panels, was used to design the Gr/PI configurations shown.

Details of the simplified-buckling-analysis optimization computer program are given in references 18 and 19, and details of PASC0 (Panel Analysis and Sizing Code) are given in reference 20. Both programs require the user to model the panel cross section as an assembly of flat plate elements and allow the user to select minimum gage and maximum strain constraints for each lamina. The simplified-buckling-analysis optimization program allowed wide column buckling of the panel and local buckling of flat plate elements in which each flat plate element was assumed to be infinitely long and simply supported. The PASC0 computer program included a sophisticated buckling analysis that provided exact buckling solutions for the panel within the limits of linear-elastic thin-plate theory, thus allowing analytical optimization of panels susceptible to rolling modes, such as blade-stiffened panels. Other design considerations available in PASC0 include a bow-type geometric panel imperfection, and the Tsai-Wu failure criterion for each lamina with the F_{12} term set equal to zero as discussed in reference 21.

The skin core heights calculated by the optimization programs are less than that required to support the design loads in the honeycomb-sandwich-panel skin configurations subject to local skin buckling because the buckling analyses in the optimization programs do not consider transverse shearing effects. However, additional buckling analyses that include transverse shearing effects were made on those optimized panel designs selected for fabrication to determine the additional core height required to prevent buckling at the design load.

Several of the structurally efficient panel designs were fabricated for experimental studies to determine panel local buckling behavior and failure

characteristics. The following sections present results from these analytical and experimental studies.

Titanium Panels

Hat-stiffened titanium panel designs, suitable for use with the weld-braze joining process, were developed using the simplified-buckling-analysis optimization program. Results from the analysis of titanium panels are shown in figure 6 in terms of panel mass parameter W/AL and panel load parameter N_x/L . Details of these results are presented in reference 9. The results for titanium serve as a basis of comparison between the mass of titanium panels and the mass of various composite panel concepts. No experiments were performed to verify analytical results for the titanium panels.

Aluminum-Matrix Composite Panels

Analytical results. - The simplified-buckling-analysis optimization program (refs. 18 and 19) was also used to develop designs for hat-stiffened Bsc/Al panels (ref. 9) and ticlad Bsc/Al panels. Results from these designs are shown in figure 6 in terms of the panel mass and load parameters. The mass of the hat-stiffened honeycomb-core sandwich panel designs shown in figure 6 includes the mass of braze material in the skin as a non-structural mass.

The results indicate Bsc/Al composite panels may be 50 percent lighter than titanium panels, and the use of a honeycomb-sandwich-panel skin results in a 10- to 20-percent decrease in mass when compared to a stiffened-sheet panel. Also, ticlad Bsc/Al designs with honeycomb-sandwich-panel skins are mass competitive with Bsc/Al stiffened-sheet panels.

Examination of panel designs at a load parameter value of 2.07 MPa (300 psi) indicates that the ratio of skin mass to stiffener mass is approximately 55/45 for the ticlad Bsc/Al hat-stiffened honeycomb-sandwich panel and approximately 38/62 for the Bsc/Al hat-stiffened-sheet panel. The effect of using the honeycomb-sandwich-panel skin is to reduce stiffener mass per unit area by increasing the stiffener spacing. For a given panel width, therefore, fewer stiffeners are required with the honeycomb-sandwich-panel skin.

Fabrication and tests of stiffened-sheet panels. - Stiffened-sheet panels corresponding to a N_x/L design value of 2.07 MPa (300 psi) and corresponding to a full-scale, simply supported panel length of 76.2 cm (30 in.) were selected for fabrication and test to determine local buckling characteristics of the panels. The panel skin material was a $[\pm 45/0_3/\mp 45]_T$ Bsc/Al laminate. Panel stiffeners were fabricated using a hot forming technique from unidirectional B/Al material (the stiffness properties of B/Al are nearly equal to those of Bsc/Al). Skin and stiffeners were joined using either spotwelding or diffusion bonding. The panels were as identical as manufacturing tolerances allowed except for the joining method used for the stiffener attachment. Also, the stiffener attachment flanges of the diffusion-bonded panels were slightly narrower than those of the spotwelded

panels. This difference resulted in a slightly narrower configuration for the diffusion-bonded panels. The panel widths and lengths were 23.2 by 38.1 cm (9.12 by 15.0 in.) for the spotwelded panels and 21.4 by 38.1 cm (8.42 by 15.0 in.) for the diffusion bonded panels.

Test results from stiffened-sheet panels. - Test results for the stiffened-sheet panels are shown in figure 7 in terms of the mass and load parameters. The solid line in figure 7 is the analytical curve for Bsc/Al taken from figure 6, the circle indicates the design point at the value of the load parameter previously indicated, and the squares and triangles are test results obtained from measured failure loads and panel mass from the spotwelded and diffusion-bonded panels, respectively. Buckling and failure occurred nearly simultaneously for all results shown.

The test panels are heavier than the mass indicated by the design point because the analytical model did not include the mass of the stiffener attachment flanges. The low values of failure loading shown for two of the diffusion-bonded panels resulted from premature joint failures. Failures of the remaining panels occurred at a strain level of approximately 0.003 and were typified by a wrinkling mode failure in the skin in which the skin buckled away from the stiffeners across the entire width of the panel as shown in figure 8. For the spotwelded panels, the wrinkling mode had a halfwave length equal to several spotweld spacing lengths. Observations made of the spotwelded panels after failure indicated several spotweld failures in the buckled skin region and indicated that the stiffeners underwent large strains transverse to the fibers in the bend radii adjacent to the attachment flanges to accommodate the skin deformation (see fig. 8). This buckling mode was not considered in the simplified-buckling-analysis optimization program and was not the critical mode predicted in BUCLASP 2 analyses of the panels. Similar wrinkling mode failures have previously been observed, however, and are discussed in reference 22.

Fabrication and tests of hat-stiffened honeycomb-core sandwich panels. - Tielad Bsc/Al panels with honeycomb-sandwich-panel skins corresponding to a N_x/L design value of 2.07 MPa (300 psi) and a full-scale, simply supported panel length of 76.2 cm (30 in.) were selected for fabrication and tests to determine the local buckling characteristics of the panels. The panel skin consisted of tielad Bsc/Al cover sheets brazed to 6.35 mm (0.25 in.) titanium honeycomb-core material having a density of 149 kg/m³ (9.3 lbm/ft³). The titanium in the tielad Bsc/Al was 0.076 mm (0.003 in.) thick and was diffusion bonded to each side of the Bsc/Al composite in the cover sheets and stiffener material during the consolidation process. A [± 45]_T Bsc/Al laminate (an unsymmetric laminate) was used in each cover sheet, and ten layers of unidirectional Bsc/Al were used in the hat stiffeners. The hat stiffeners were hot formed after composite consolidation. Each panel was fabricated in a two step braze operation. In the first braze temperature cycle the cover sheets were brazed to the honeycomb core using 0.127 mm (0.005 in.) thick aluminum braze material between each cover sheet and core. The resulting honeycomb-sandwich-panel skin was a balanced and symmetric laminate. In the second braze temperature cycle, the tielad Bsc/Al hat stiffeners were brazed to the skin. The panel widths and lengths were 55.4 by 61.0 cm (21.8 by 24.0 in.).

Test results from hat-stiffened honeycomb-core sandwich panels. - Test results for the hat-stiffened honeycomb-core sandwich panels are shown in figure 9 in terms of the mass and load parameters. The solid line in figure 9 is the analytical curve for ticlad Bsc/Al taken from figure 6, and the squares are test results obtained from measured failure loads and panel mass.

The test panels are heavier than the mass indicated by the design point because the analysis model did not include the mass of the stiffener attachment flanges. In addition, the titanium honeycomb-core material used in the test panels was twice the height designated by the analysis program because smaller core heights were commercially unavailable and also to compensate for out-of-plane shear deformation as previously discussed.

Failure of these panels, unfortunately, was immediately preceded by brooming of the hat stiffener ends. A preliminary study of moiré-fringe and strain-gage data taken during the tests indicates no skin or stiffener buckling prior to brooming of the hat stiffeners. The failure strains of these panels are approximately 0.005, or 67 percent higher than the failure strains of the stiffened-sheet panels.

Panel failures were characterized by wrinkling of the skin across the entire width of the panel with some fracturing of the braze material in the skin and crimping type failures of the entire stiffener at the lengthwise location of the skin wrinkle. Visual observations of the failed panels indicated that the titanium was pulled away from the ticlad Bsc/Al composite material in only a small area of one stiffener. In addition, matrix dominated modes of failure were not observed in the ticlad Bsc/Al panels.

Comparison between the test results of the stiffened-sheet panels and the stiffened honeycomb-sandwich panels indicates that nearly equal values of mass and load parameters were attained by both types of panels. However, the stiffened honeycomb-sandwich panel (ticlad Bsc/Al panel) experimental failure loads may be conservative because of brooming.

Graphite/Polyimide Composite Panels

Analytical results. - The PASCO computer program was used to design Gr/PI composite panels. The configurations studied were either stiffened-sheet panels or stiffened honeycomb-core sandwich panels. Both blade stiffeners and hat stiffeners were studied. The blade stiffener used in the analysis is a built-up stiffener using a honeycomb core. Stiffeners of this type were previously examined for graphite-epoxy compression panels and the results of the study are presented in reference 23. Results from the present study are shown in figure 10 in terms of the panel mass and load parameters. The hat-stiffened titanium panel curve is from figure 6 and is included for comparison with the Gr/PI panel curves. Details of the study are given in reference 10. The mass of adhesive required in panel fabrication is not included in the mass parameter.

The PASCO program includes an effect of initial geometric imperfection in the form of a bow over the length of the panel. For the results shown in

figure 10, panel bows with amplitudes of ± 1 percent of panel length were included in the optimization analysis. In addition, the Tsai-Wu failure criterion constrains the designs to longitudinal strains less than 0.004. This value of strain may be in excess of the allowable strain determined by impact criteria as discussed in reference 24. However, when an impact sensitivity criterion is established, it can easily be incorporated into the design procedure.

The results shown in figure 10 indicate Gr/PI composite panels may be 50 percent lighter than titanium panels, or approximately the same mass as the aluminum-matrix composite panels for the room temperature conditions of this study. Examination of panel designs at a load parameter value of 2.30 MPa (333 psi) indicates that the ratio of skin mass to stiffener mass is approximately 70/30 for the blade-stiffened honeycomb-sandwich panel and approximately 45/55 for the blade-stiffened stiffened-sheet panel. The effect of using the honeycomb-sandwich-panel skin is to reduce stiffener mass per unit area by increasing the stiffener spacing. Thus, for a given panel width, fewer stiffeners are required with the honeycomb-sandwich-panel skin.

Comparison of panel mass and load parameters between the present study and those of reference 23 indicates larger values of the mass parameter are required by the present analysis for any given value of load parameter. This results, in part, from the minimum gage constraints (for the lower values of load parameter) and from the Tsai-Wu failure criterion (for the higher values of load parameter) used in the present analysis.

Fabrication of Gr/PI panels.- Gr/PI panels corresponding to a N_x/L design value of 2.30 MPa (333 psi) and a full-scale, simply supported panel length of 76.2 cm (30 in.) were selected for fabrication and test to determine the local buckling characteristics of the panels. The design point is indicated by the circle in figure 10. The honeycomb core sandwich panel skin laminates are $[\pm 45/0_n/\mp 45/HC/\pm 45/0_n/\mp 45]_T$ and the stiffened-sheet panel skin laminate is $[(\pm 45)_2/0_n/(\mp 45)_2]_T$, where the number of 0° laminae, n , are 5, 6, and 6 for the hat-stiffened honeycomb-sandwich skin, blade-stiffened honeycomb-sandwich skin and blade-stiffened sheet, respectively. The values of n are based on a lamina thickness of 0.178 mm (0.007 in.). The webs of both the hat and blade stiffeners are balanced and symmetric 45° laminates. In the design, 0° laminates are also located at the bottom and top of the stiffeners. The honeycomb-core material is a 128 kg/m^3 (8 lbm/ft^3) density glass/polyimide.

SPF/DB Titanium Panels

As mentioned previously, several fabrication and joining studies are being conducted on SPF/DB titanium stiffened and sandwich compression panels. In addition to these activities, analytical studies are being conducted to develop promising SPF/DB titanium sandwich panel configurations and compare their structural efficiencies. This section describes buckling analysis results from these studies in which a new SPF/DB titanium orthogonally-corrugated-core sandwich panel configuration is compared to

SPF/DB titanium square-cell-core and unidirectionally-corrugated-core sandwich panel configurations.

The orthogonally-corrugated-core sandwich panel configuration is shown in figure 11. This configuration is fabricated using four layers of titanium alloy sheet in which the outer layers are face sheets and the inner layers are core sheets. During the superplastic expansion process, the upper core sheet forms the array of inverted hollow pyramids shown in figure 11 and the lower core sheet forms the array of upright hollow pyramids. The two sets of pyramids become diffusion bonded to the face sheets and to each other at the edges of their triangular sides during the expansion process. Details of the core sheet and stopoff material geometries before superplastic expansion and details of sheet movement during the expansion process are given in references 25 and 26.

Preliminary buckling results for the three panel configurations are shown in figure 12 in terms of the buckling load parameter and panel aspect ratio. The curves were obtained for uniaxially loaded, simply supported panels having constant width, depth and mass per unit length. For the results shown in figure 12, the skin mass (cover sheets) was held constant at 46 percent of the total panel mass. These results indicate that orthogonally-corrugated-core sandwich panels have structural efficiencies comparable to those of square-cell-core sandwich panels and these panel configurations are more structurally efficient than unidirectionally-corrugated-core sandwich panels.

CONCLUDING REMARKS

Experience gained during fabrication and joining studies of aluminum-matrix composites led to the recommendation of ticlad Bsc/Al and brazing as the most structurally efficient combination of material and joining method for use in aluminum-matrix stiffened compression panels. In addition, these studies indicated that the buckling behavior of stiffened panels is dependent upon the method used to attach the stiffeners to the skin and strong, continuous joints produce the most structurally efficient panels. It was also found that a hot forming process could be used successfully to produce high strength Bsc/Al, ticlad Bsc/Al and B/Al hat stiffeners. However, present hot and cold forming methods for Bsc/Al, ticlad Bsc/Al and B/Al stiffeners prohibit the use of angle-ply laminates in the stiffeners.

Results from Bsc/Al stiffened compression panel experimental studies indicated that the buckling characteristics of these panels differ from predictions obtained using linear elastic analyses because of the transverse inelastic behavior of the unidirectional laminate used in the stiffeners. Preliminary results from the study on ticlad Bsc/Al indicate reasonably good agreement between analytical and experimental results in terms of mass and strength. However, buckling characteristics were not determined experimentally for these panels because brooming of the hat stiffeners occurred prior to buckling. Visual examination of the ticlad Bsc/Al panels after failure indicated that the transverse inelastic behavior in the stiffeners was much less than that observed in the Bsc/Al panels.

Analysis of Gr/PI stiffened-compression panels indicated that the mass and strength of Gr/PI panels may be comparable to those for ticlad Bsc/Al panels. In addition, analysis of SPF/DB titanium sandwich panel configurations indicates that orthogonally-corrugated-core sandwich panels have structural efficiencies comparable to that of square-cell-core sandwich panels.

REFERENCES

1. Turner, M. J.; and Hoy, J. M.: Titanium and Advanced Composite Structures for a Supersonic Cruise Arrow Wing Configuration. Proceedings of the SCAR Conference, Part 2, NASA CP-001, [1977], pp. 579-602.
2. Sakata, I. F.; and Davis, G. W.: Advanced Structures Technology Applied to a Supersonic Cruise Arrow-Wing Configuration. Proceedings of the SCAR Conference, Part 2, NASA CP-001, [1977], pp. 603-636.
3. Fischler, J. E.: Structural Design of Supersonic Cruise Aircraft. Proceedings of the SCAR Conference, Part 2, NASA CP-001, [1977], pp. 911-925.
4. Ascani, Leonard A.; and Pulley, John K.: New Advancements in Titanium Technology and Their Cost and Weight Benefits. Proceedings of the SCAR Conference, Part 2, NASA CP-001, [1977], pp. 757-782.
5. Technology Application Studies for Supersonic Cruise Aircraft: Vol. 1., NASA CR-144925, Nov. 1975.
6. Bales, Thomas T.; Royster, Dick M.; and Arnold, Winfrey E., Jr.: Development of the Weld-Braze Joining Process. NASA TN D-7281, 1973.
7. Royster, Dick M.; Wiant, H. Ross; and McWithey, Robert R.: Effects of Fabrication and Joining Processes on Compressive Strength of Boron/Aluminum and Borsic/Aluminum Structural Panels. NASA TP-1121, 1978.
8. Royster, Dick M.; McWithey, Robert R.; and Bales, Thomas T.: Fabrication and Evaluation of Brazed Titanium-Clad Borsic[®]/Aluminum Compression Panels. NASA TP-1573, 1980.
9. McWithey, Robert R.: Analytical Structural Efficiency Studies of Borsic/Aluminum Compression Panels. NASA TN D-8333, 1976.
10. McWithey, Robert R.; Camarda, Charles J.; and Weaver, Gerald G.: Design Considerations for Compression Panels at Elevated Temperature. Graphite/Polyimide Composites, NASA CP-2079, 1979, pp. 319-337.
11. Ko, William L.: Elastic Constants for Superplastically Formed/Diffusion-Bonded Sandwich Structures. AIAA Paper No. 79-0756, AIAA/ASME/ASCE/AHS 20th Structures, Structural Dynamics and Materials Conference, St. Louis, Mo., April 1979.

12. Royster, Dick M.; Wiant, H. Ross; and Bales, Thomas T.: Joining and Fabrication of Metal-Matrix Composite Materials. NASA TM X-3282, 1975.
13. Bales, Thomas T.; Wiant, H. Ross; and Royster, Dick M.: Braze Borsic/Aluminum Structural Panels. NASA TM X-3432, 1977.
14. Tripp, L. L.; Tamekuni, M.; and Viswanathan, A. V.: User's Manual- BUCLASP 2: A Computer Program for Instability Analysis of Biaxially Loaded Composite Stiffened Panels and Other Structures. NASA CR-112226, 1973.
15. Herakovich, C. T.; Davis, J. G., Jr.; and Viswanathan, C. N.: Tensile and Compressive Behavior of Borsic/Aluminum. Composite Materials: Testing and Design (Fourth Conference), ASTM STP 617, 1977, pp. 344-357.
16. Graphite/Polyimide Composites, NASA CP-2079, 1979.
17. Fischler, J. E.: Opportunities for Structural Improvements for an Advanced Supersonic Transport Vehicle. Supersonic Cruise Research '79, NASA CP-2108, 1980, pp. 589-616.
18. Agarwal, Banarsi; and Davis, Randall C.: Minimum-Weight Designs for Hat-Stiffened Composite Panels Under Uniaxial Compression. NASA TN D-7779, 1974.
19. Stroud, W. Jefferson; and Agranoff, Nancy: Minimum-Mass Design of Filamentary Composite Panels Under Combined Loads: Design Procedure Based on Simplified Buckling Equations. NASA TN D-8257, 1976.
20. Anderson, M. S.; and Stroud, W. J.: A General Panel Sizing Computer Code and Its Application to Composite Structural Panels. AIAA Paper No. 78-467, AIAA/ASME 19th Structures, Structural Dynamics and Materials Conference, Bethesda, Md., April 1978.
21. Narayanaswami, R.; and Adelman, Howard M.: Evaluation of the Tensor Polynomial and Hoffman Strength Theories for Composite Materials, J. of Composite Materials, Vol. 11, Oct. 1977, pp. 366-377.
22. Gerard, George: Handbook of Structural Stability. Part V - Compressive Strength of Flat Stiffened Panels. NACA TN 3785, 1957.
23. Stein, Manuel; and Williams, Jerry G.: Buckling and Structural Efficiency of Sandwich-Blade Stiffened Composite Compression Panels. NASA TP-1269, 1978.
24. Garcia, Ramon; and Rhodes, Marvin D.: Effects of Low-Velocity Impact on Gr/PI Compression Laminates. Graphite/Polyimide Composites, NASA CP-2079, 1979, pp. 239-248.
25. Ko, W. L.: Superplastically-Formed/Diffusion-Bonded Metallic Structures. NASA Patent Application, Case No. FRC-11026, May 1979.

26. Ko, W. L.: Structural Properties of Superplastically-Formed/Diffusion-Bonded Orthogonally-Corrugated-Core Sandwich Plates. AIAA Paper No. 80-0304, AIAA 18th Aerospace Sciences Meeting, Pasadena, Calif., Jan. 1980.

TABLE I. - Materials and Processes Used in Aluminum Matrix Composite Fabrication and Joining Study

SKIN MATERIAL	STIFFENER		JOINING PROCESS ^b
	MATERIAL	FABRICATION PROCESS ^a	
B/Al	B/Al	C, H, E	1, 2, 3, 4
Ti	B/Al	C, H, E	1, 2, 3, 4
Bsc/Al	Bsc/Al	H	1, 5
Ti	Bsc/Al	H	1, 5
Ticlad Bsc/Al	Ticlad Bsc/Al	H	5

^aFabrication process code: C = cold formed; H= hot formed; and E = eutectic bonded.

^bJoining process code: 1 = spotwelded; 2 = bolted; 3 = diffusion bonded; 4 = adhesive bonded; and 5 = brazed.

TABLE II. - Material Properties used in BUCLASP 2 Analyses

Titanium:

Young's modulus ----- 121 GPa (17.6 x 10⁶ psi)
 Shear modulus ----- 46.7 GPa (6.77 x 10⁶ psi)
 Poisson's ratio ----- 0.30

Metal-matrix composite:

Longitudinal Young's modulus^a----- 228 GPa (33.0 x 10⁶ psi)
 Transverse Young's modulus----- 131 GPa (19.0 x 10⁶ psi)
 Major Poisson's ratio ----- 0.26
 Shear modulus ----- 57.2 GPa (8.3 x 10⁶ psi)

^aDetermined from panel test data.

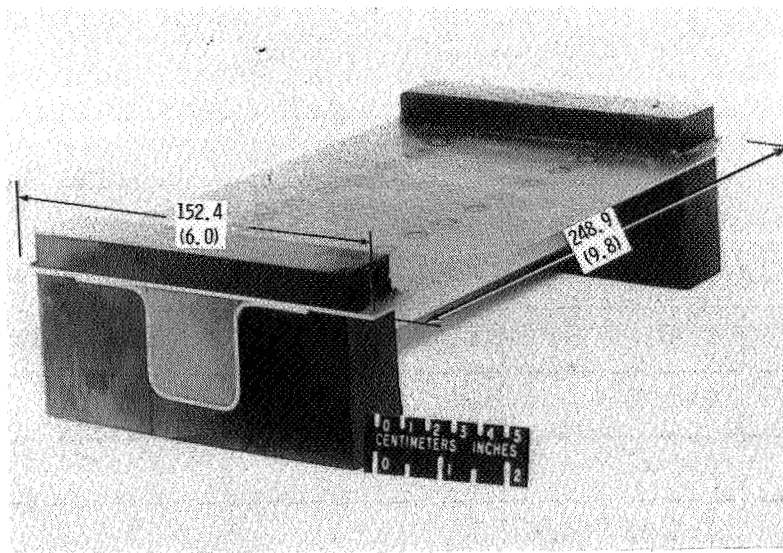


Figure 1.- Typical panel configuration used in fabrication and joining studies. Dimensions given in millimeters (inches).

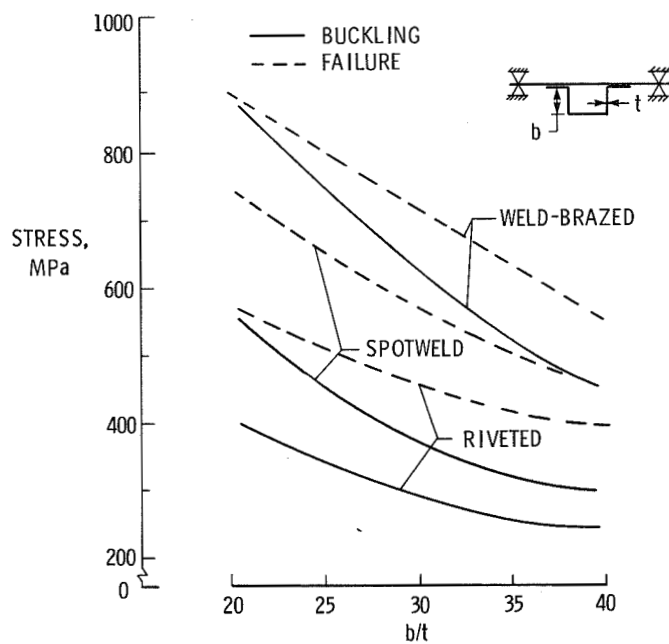


Figure 2.- Effect of joining processes on buckling and failure stresses of titanium skin-stringer panels.

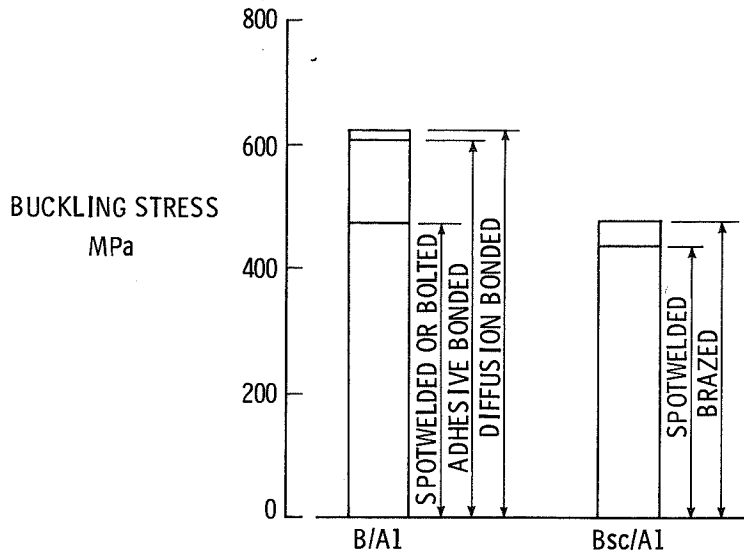


Figure 3.- Effect of joining method on panel buckling strength of hat-stiffened aluminum-matrix composite panels for $b/t = 30$.

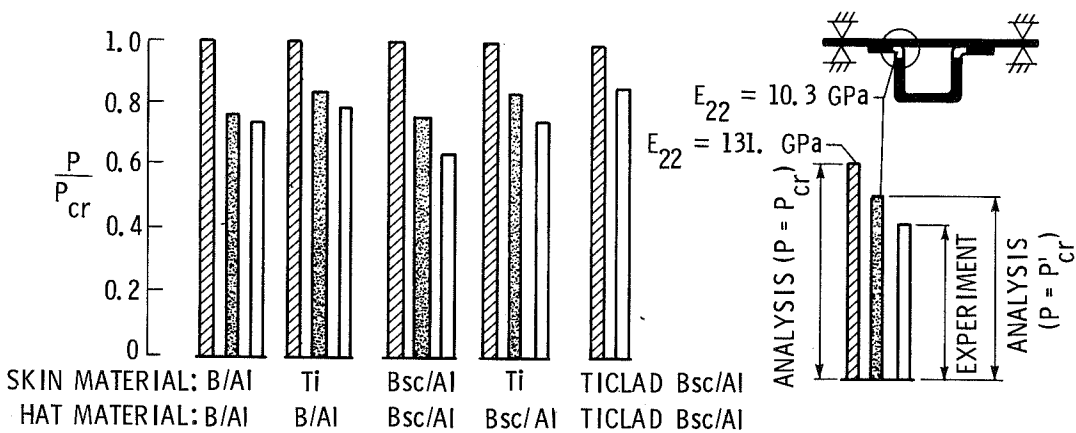

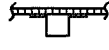
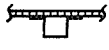



Figure 4.- Comparison between analytical and experimental buckling loads of aluminum panels with continuous joints.

MATERIAL	PANEL CONFIGURATION ^a	OPTIMIZATION PROGRAM
TITANIUM Bsc/Al TICLAD Bsc/Al	 	SIMPLIFIED BUCKLING ANALYSIS (refs. 18 & 19)
Gr/PI	 	PASCO (ref. 20)

^a PANEL CONFIGURATION DESCRIPTIONS





-  HAT-STIFFENED SHEET PANEL
-  HAT-STIFFENED HONEYCOMB-CORE SANDWICH PANEL
-  BLADE-STIFFENED SHEET PANEL
-  BLADE-STIFFENED HONEYCOMB-CORE SANDWICH PANEL

Figure 5.- Stiffened panel design concepts examined in present analytical study.

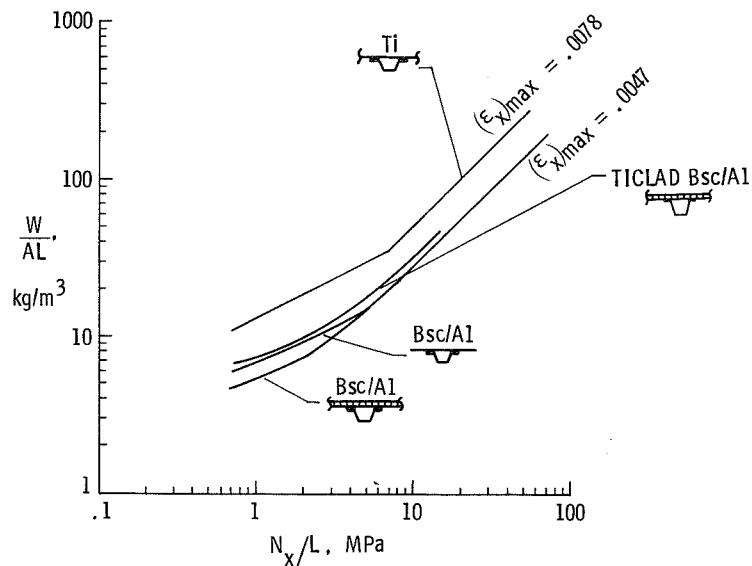


Figure 6.- Typical results from analytical study of full-scale compression panels. $(\epsilon_x)_{max}$ is the maximum longitudinal strain.

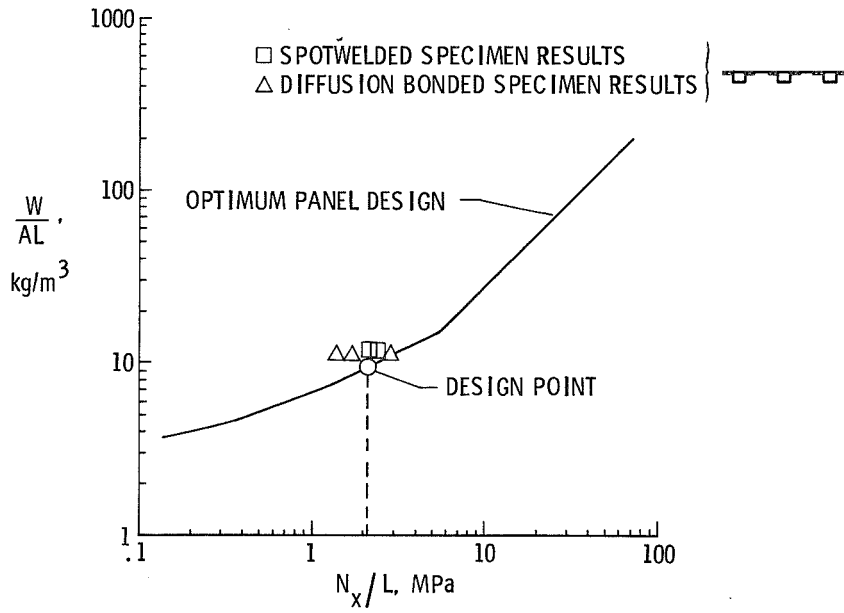
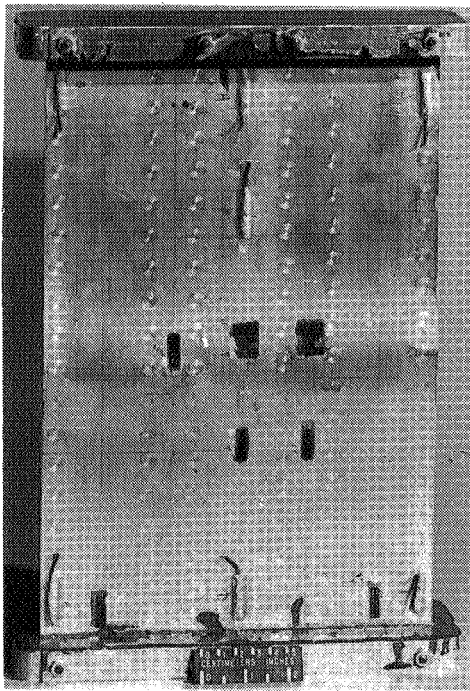
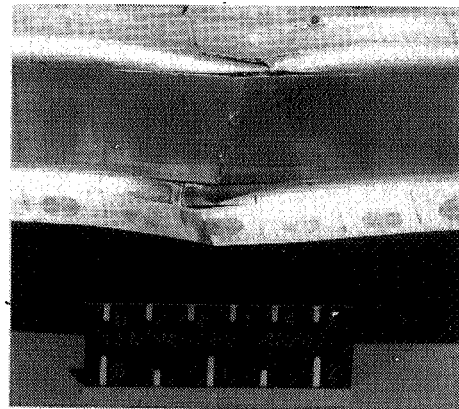


Figure 7.- Comparison between full-scale panel analysis and local buckling tests for hat-stiffened panels with Bsc/Al skins and B/Al stiffeners.



(a) Skin failure.



(b) Stiffener failure.

Figure 8.- Typical local buckling failure of panels with Bsc/Al skins and B/Al stiffeners.

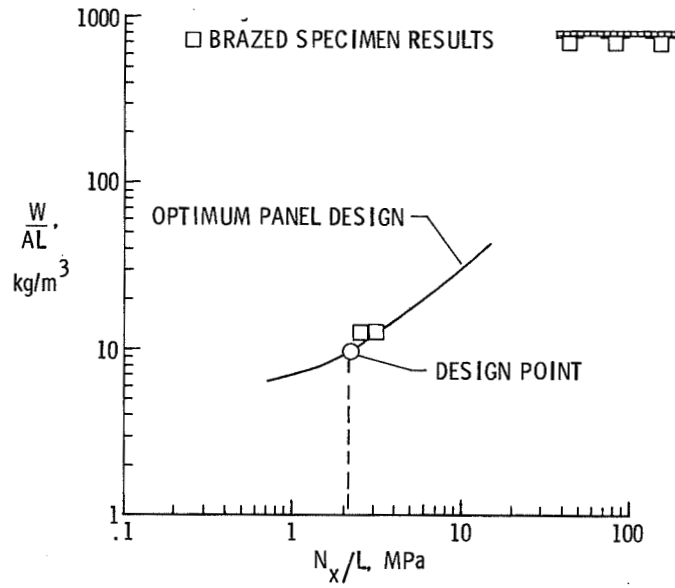


Figure 9.- Comparison between full-scale panel analysis and local buckling test for ticlad Bsc/Al panels.

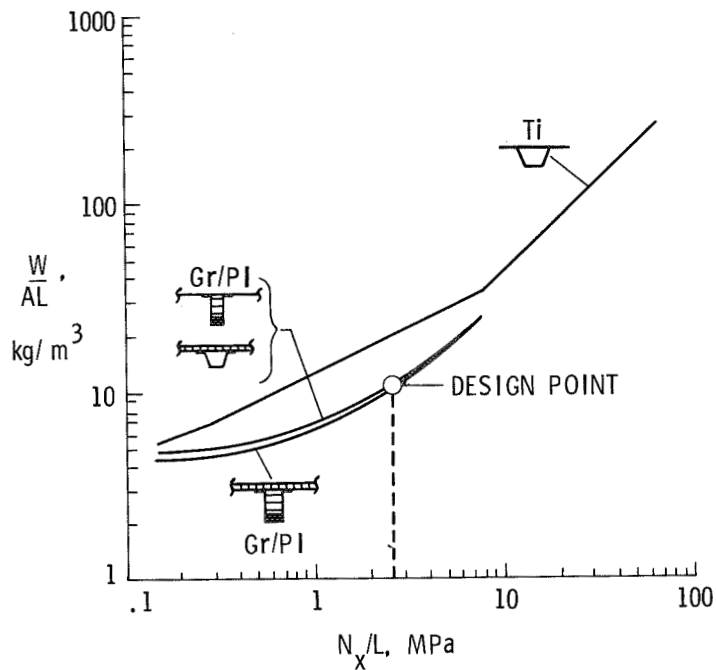


Figure 10.- Typical results from analytical study of full-scale Gr/PI composite panels.

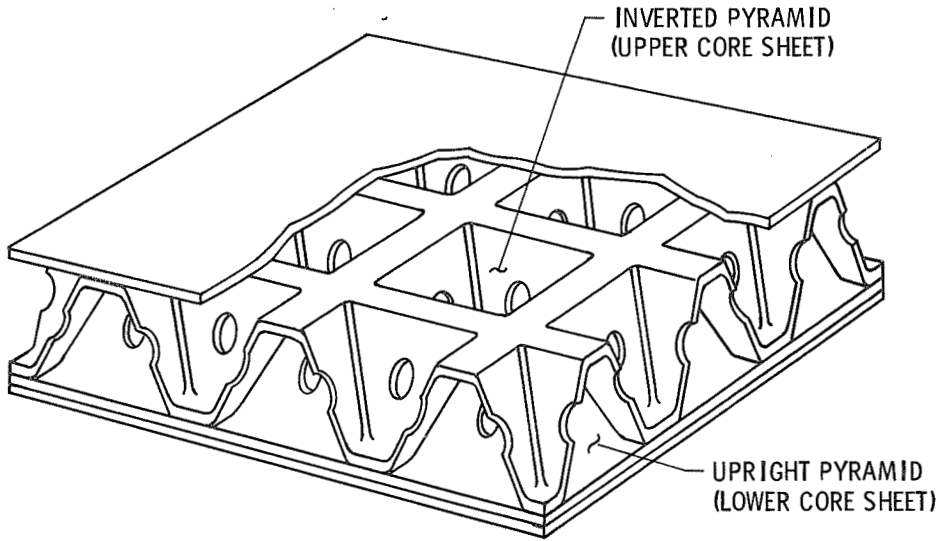


Figure 11.- Geometry of SPF/DB orthogonally-corrugated-core sandwich panel.

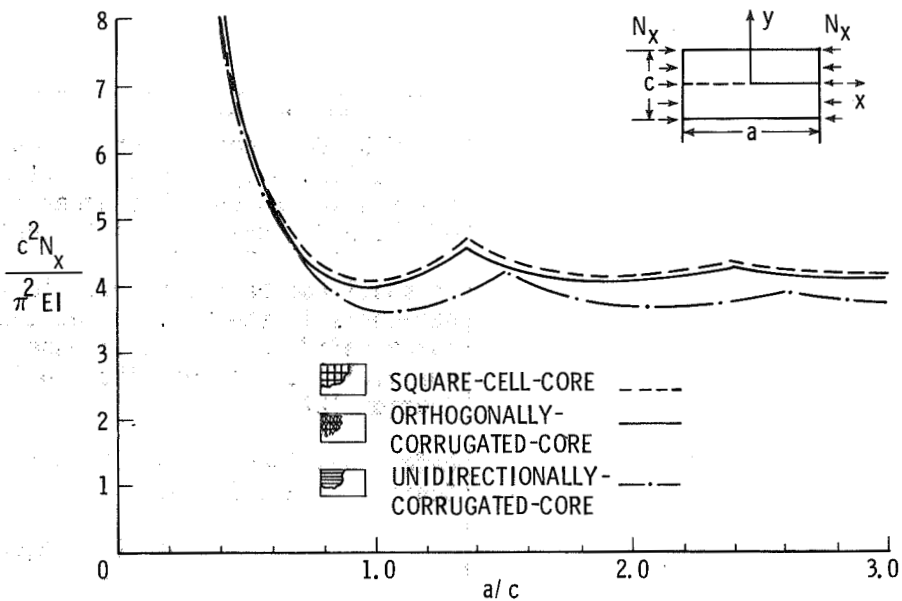


Figure 12.- Buckling curves for SPF/DB titanium sandwich panels.

1. Report No. NASA TP-1617	2. Government Accession No.	3. Recipient's Catalog No.	
4. Title and Subtitle COMPRESSION PANEL STUDIES FOR SUPERSONIC CRUISE VEHICLES		5. Report Date March 1980	
		6. Performing Organization Code	
7. Author(s) Robert R. McWithey, Dick M. Royster, and William L. Ko		8. Performing Organization Report No. L-13525	
		10. Work Unit No. 533-01-13-06	
9. Performing Organization Name and Address NASA Langley Research Center Hampton, VA 23665		11. Contract or Grant No.	
		13. Type of Report and Period Covered Technical Paper	
12. Sponsoring Agency Name and Address National Aeronautics and Space Administration Washington, DC 20546		14. Sponsoring Agency Code	
		15. Supplementary Notes Robert R. McWithey and Dick M. Royster: Langley Research Center. William L. Ko: Dryden Flight Research Center.	
16. Abstract <p>Results of analytical and experimental studies are summarized for titanium, boron-fiber-reinforced aluminum-matrix composite, Borsic®-fiber-reinforced aluminum-matrix composite, and titanium-sheathed Borsic-fiber-reinforced aluminum-matrix composite stiffened panels. The results indicate that stiffened panels with continuous joints (i.e., brazed, diffusion-bonded or adhesive-bonded joints) are more structurally efficient than geometrically similar panels with discrete joints (i.e., spotwelded or bolted joints). In addition, results for various types of fiber-reinforced aluminum-matrix stiffened panels indicate that titanium-sheathed Borsic-fiber-reinforced aluminum-matrix composite panels are the most structurally efficient. Analytical results are also presented for graphite-fiber-reinforced polyimide-matrix composite stiffened panels and superplastically formed and diffusion-bonded titanium sandwich panels.</p>			
17. Key Words (Suggested by Author(s)) Composite Compression panel Superplastic forming Diffusion bonding			
19. Security Classif. (of this report) Unclassified	20. Security Classif. (of this page) Unclassified	21. No. of Pages 21	22. Price